J. Fluid Mech. (1997), *vol.* 349, *pp.* 191–219. Printed in the United Kingdom

Premixed flame–wall interaction in a turbulent channel flow: budget for the flame surface density evolution equation and modelling

By G. BRUNEAUX[1], T. POINSOT[2]† AND J. H. FERZIGER[3]

[1]Institut Francais du Pétrole, and Centre de Recherche sur la Combustion Turbulente, BP 311, 92506 Rueil Malmaison Cedex, France

[2]Institut de Mécanique des Fluides de Toulouse and CERFACS; Av. C. Soula, 31400 Toulouse Cedex, France
e-mail: poinsot@cerfacs.fr

[3]Mechanical Engineering Department, Stanford University, Stanford, CA 94305, USA

(Received 20 May 1996 and in revised form 3 June 1997)

Turbulent premixed flame propagation in the vicinity of a wall is studied using a three-dimensional constant-density simulation of flames propagating in a channel. The influence of the walls is investigated in terms of the flamelet approach, where flamelet speed and flame surface density transport are used to describe the flame. The walls have constant temperature and lead to flamelet quenching for sufficiently small wall–flame distances. Starting from the exact evolution equation for the surface density of propagating interfaces (Trouvé & Poinsot 1994; Candel & Poinsot 1990; Pope 1988), a budget for the flame surface density equation is presented before, during, and after the interaction with the wall. Before the flame interacts with the wall, flame propagation is controlled by a balance between surface production and annihilation. During the interaction, high flame surface density gradients near the wall are responsible for the predominance of the transport terms. Closures of all terms of the flame surface density equation are proposed. These models are based on flamelet ideas and take into account wall effects. Enthalpy loss through the wall affects flamelet speed, flamelet annihilation and flame propagation. Decrease of turbulent scales near the wall affects turbulent diffusion and flame strain. This model is compared to DNS results using two types of tests: (i) *a priori* tests, where individual terms of the modelled flame surface density equation are compared to the terms of the exact interface density propagation equation, calculated with the DNS; (ii) *a posteriori* tests, where the final model is used to obtain total reaction rate, mean fuel mass fraction, heat flux at the wall and fuel mass fraction at the wall in the configuration used in the DNS. For both types of tests the model compares well with the DNS results.

1. Introduction

Understanding and modelling of near-wall turbulence have been key issues in engineering problems and the source of an extremely abundant literature. The treatment of near-wall turbulence for non-reacting flows is still a difficult problem and quite often the limiting factor in practical predictions.

† Author to whom correspondence should be addressed.

Wall problems become more critical in chemically reacting flows. Combustion is strongly influenced by the presence of walls which may cause, for example, flame quenching. The flame also has a significant effect on the flow near the wall as well as on the heat flux to the wall (Clendening, Shackleford & Hilyard 1981; Lu *et al.* 1990; Ezekoye & Greif 1993; Ezekoye, Greif & Lee 1992; Popp & Baum 1997). Heat fluxes of the order of 1 $\mathrm{MW\,m^{-2}}$ may be reached in practical situations and prediction of wall temperatures required for structure design may become hazardous.

Flame–wall interaction in laminar flows has been extensively studied both experimentally and numerically (Jarosinski 1986; Clendening *et al.* 1981; Huang, Vosen & Grief 1986; Vosen, Greif & Westbrook 1984; Ezekoye & Greif 1993; Ezekoye *et al.* 1992; Vlachos 1995, 1996). However, except for the pioneering numerical work of Westbrook *et al.* 1981 and the more recent work of Popp & Baum (1997) who used complex chemistry schemes, most modelling has been based on simple one-step chemical reactions. At the moment, the effects of surface chemistry or adsorption are not completely understood (Popp & Baum 1997). More importantly, there are important variations in experimental results which lead to difficulties in interpreting the quality of models (Ezekoye & Greif 1993; Ezekoye *et al.* 1992; Popp & Baum 1997). This is due to the difficulty of performing measurements close to walls. In practice, only heat fluxes to the wall have been measured and even they exhibit large uncertainty margins.

In turbulent flows, modelling of flame–wall interactions has not yet been recognized as an important issue. Except for some simple attempts (Jennings & Morel 1990; Poinsot, Haworth & Bruneaux 1993), most models for turbulent premixed combustion did not use specific corrections for near-wall effects. In practice, very little is known about the effects of turbulence during flame–wall interaction.

The interaction between flame, wall, and turbulence is quite complex and involves multiple paths. The wall quenches flame elements close to it via heat losses and fuel depletion (walls are generally much colder than the flame). The wall also limits the flame wrinkling. Indirectly, it affects the turbulent flame because it strongly modifies the turbulence acting on the flame when the flame enters the near-wall region. The flame affects the turbulence due to the dilatation generated at the flame front and the increase of viscosity in the burnt gases. Obviously these coupled interactions lead to phenomena which are difficult to model.

One possible way to formulate the problem in the context of modelling is to use the classical flamelet approach (Cant, Pope & Bray 1990; Candel *et al.* 1990). In this approach, the flame–flow interaction is described in terms of the product of two quantities: a local consumption speed that characterizes the inner flame structure, and a surface density that characterizes flame wrinkling.

The mean reaction rate, which is the central quantity in most turbulent combustion models, can then be written as proposed by Trouvé & Poinsot (1994):

$$\overline{\dot{\omega}}_R = \rho_1^0 Y_1^0 \langle s_l \rangle_S \, \Sigma, \tag{1}$$

where $\Sigma = \langle \Sigma' \rangle$ is the interface surface density between fresh and burnt gases (Σ' is the local surface to volume ratio). The $\langle\,\rangle_S$ operator designates a surface mean defined (Pope 1988) for any function Q by $\langle Q \rangle = \langle Q\Sigma' \rangle / \Sigma$ so that $\langle s_l \rangle_S = \langle s_l \Sigma' \rangle / \Sigma$ is the surface-averaged consumption speed; $s_l = 1/(\rho_1^0 Y_1^0) \int \dot{\omega}_R \, \mathrm{d}n$ is the local consumption speed (reaction rate integrated along the local normal to the flame); $\langle\,\rangle$ denotes a standard ensemble averaging; ρ_1^0 is the initial density in the fresh gases and Y_1^0 is the initial fuel mass fraction in the fresh gases.

Two quantities must be determined to make equation (1) useful: (i) the mean

consumption speed of flamelets $\langle s_l \rangle_S$ and (ii) the flame surface density Σ. We expect both quantities to be affected by the presence of the wall because of the multiple interactions described above.

(i) In general, s_l and the local flame structure are modified by the turbulent flow (owing to flame stretch) and by heat losses (owing either to the presence of walls or to radiative losses). Many recent DNS results (Trouvé & Poinsot 1994; Haworth & Poinsot 1992; Baum *et al.* 1994) have shown that, far from walls, s_l remains approximately constant over a wide range of turbulence conditions. However, in the presence of enthalpy losses through wall heat losses and fuel depletion, the local flame speed is affected and decreases (Williams 1985; Wichman & Bruneaux 1995). Finally, close enough to the wall, flame elements are quenched. This occurs when the distance between wall and flame is of the same order as the quenching distance δ_Q. This distance is usually expressed in terms of a Péclet number defined by $Pe_Q = \delta_Q/d$, where d is a flame reference length defined by $d = \lambda_1/(\rho_1 c_p s_l^0)$ and subscript 1 refers to fresh gas and s_l^0 is the unstrained planar flame speed. The Péclet number may depend on configuration and varies between 3 and 7. We will focus on this effect throughout this paper and neglect the effects of stretch on s_l.

(ii) An exact transport equation can be derived to obtain the interface surface density Σ. It is derived from the equation for the tranport of a self-propagating surface (Trouvé & Poinsot 1994; Candel & Poinsot 1990; Pope 1988):

$$\frac{\partial \Sigma}{\partial t} + \frac{\partial}{\partial x_i} \langle \boldsymbol{v} \rangle_S \Sigma + \frac{\partial}{\partial x_i} \langle \omega \boldsymbol{n} \rangle_S \Sigma = \langle a_T \rangle_S \Sigma + 2 \langle \omega k_m \rangle_S \Sigma, \tag{2}$$

where $\boldsymbol{v}$ is the fluid velocity vector, $\boldsymbol{n}$ is the flame normal, ω is the propagation speed of the surface relative to the flow, $\langle a_T \rangle_S = \langle \nabla \cdot \boldsymbol{v} - \boldsymbol{n}\boldsymbol{n} : \nabla \boldsymbol{v} \rangle_S$ is the strain acting on the interface, and $k_m = \frac{1}{2} \nabla \cdot \boldsymbol{n}$ is the surface curvature. The two convective terms on the left-hand side of (2) are the transport terms due to convection by the flow and flame propagation respectively. The terms on the right-hand side are the stretch terms relative to flame straining by turbulence, and the combined effect of flame curvature and propagation. Most of the effects mentioned above (the decrease of turbulent scales near the wall and the effect on flame wrinkling and turbulent transport, the decrease of local flame propagation speed due to quenching, the geometrical limitation induced by the wall on flame curvature, etc.) can be described in terms of their influence on the various terms of the interface surface density equation (2).

The objectives of this research are to study those phenomena qualitatively and quantitatively using three-dimensional constant-density direct numerical simulations (DNS). We will perform a DNS of flames interacting with walls in controlled turbulence and exploit this data using (2) to understand the interaction and to model it. A budget of all terms of (2) will be constructed to illustrate the importance of the various mechanisms.

Two-dimensional variable-density DNS of flames interacting with walls in decaying turbulence (Poinsot *et al.* 1993) have already led to a basic understanding and to a first flame–wall interaction model (FIST). However, limitations due to decaying two-dimensional turbulence revealed a need for a better resolved wall–turbulence–flame interaction. The three-dimensional DNS code used here was initially developed by Bruneaux *et al.* (1996). In the initial paper, both variable- and constant-viscosity calculations were performed and compared. Here we will limit ourselves to constant-viscosity cases. Under this assumption (and the assumption of constant density) the flame does not affect the flow through viscosity changes or flow acceleration. This simplified configuration is more suitable to a study of the wall effects on the flame

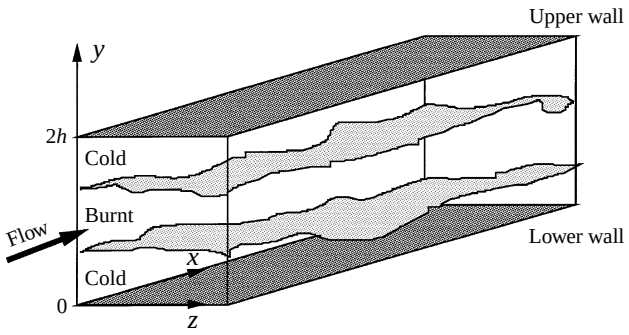

FIGURE 1. Configuration for direct numerical simulation of flame–wall interaction.

since the turbulence is stationary and well-known. We believe that these assumptions are not too limiting since previous results (three-dimensional variable viscosity and constant density (Bruneaux *et al.* 1996) and two-dimensional variable viscosity and density simulation (Poinsot *et al.* 1993) showed the preponderance of turbulence in the fresh gases. Differences between two- and three-dimensional DNS were also described by Bruneaux *et al.* (1996).

All DNS presented here use a simple chemistry assumption where chemical reaction is controlled by one irreversible reaction $Fuel \rightarrow Products$. Computations including detailed chemistry (but only in one dimension) may be found in the work of Popp & Baum (1995) and Westbrook, Adamczyk & Lavoie (1981).

We will first recall the characteristics of the database used for this work in §2.1. A detailed study of the Σ-equation terms will then be presented in §3 where the budget of the equation is presented. Finally models for all terms of the Σ-equations (including wall effects) are presented.

2. Direct numerical simulation of flame–wall interaction

2.1. *Configuration*

The simulation used in this work has been presented by Bruneaux *et al.* (1996). A three-dimensional direct numerical simulation of the turbulent flow in a channel is used to generate the baseline flow. A slab of burnt gases is introduced at the initial time near the centreplane of the channel. This slab generates two flames which propagate towards the walls (see figure 1). Constant density and viscosity assumptions are used. Variable-viscosity calculations were also performed by Bruneaux *et al.* (1996) but a constant-viscosity assumption allows a stationary flow field which is more useful for modelling purposes.

The reaction is represented by a simple one-step mechanism, corresponding, for example, to lean combustion in which fuel is the limiting factor in determining the reaction rate (Williams 1985). The reaction rate $\dot{\omega}_R$ is expressed as

$$\dot{\omega}_R = \rho \; Y_F B \exp\left(-\frac{T_a}{T}\right), \tag{3}$$

where Y_F is the mass fraction of the deficient reactant (fuel), B is the pre-exponential factor and T_a is the activation temperature.

The work of Bruneaux *et al.* (1996) was focused on individual realizations of premixed flame–wall interaction phenomena. A typical result of their DNS is given

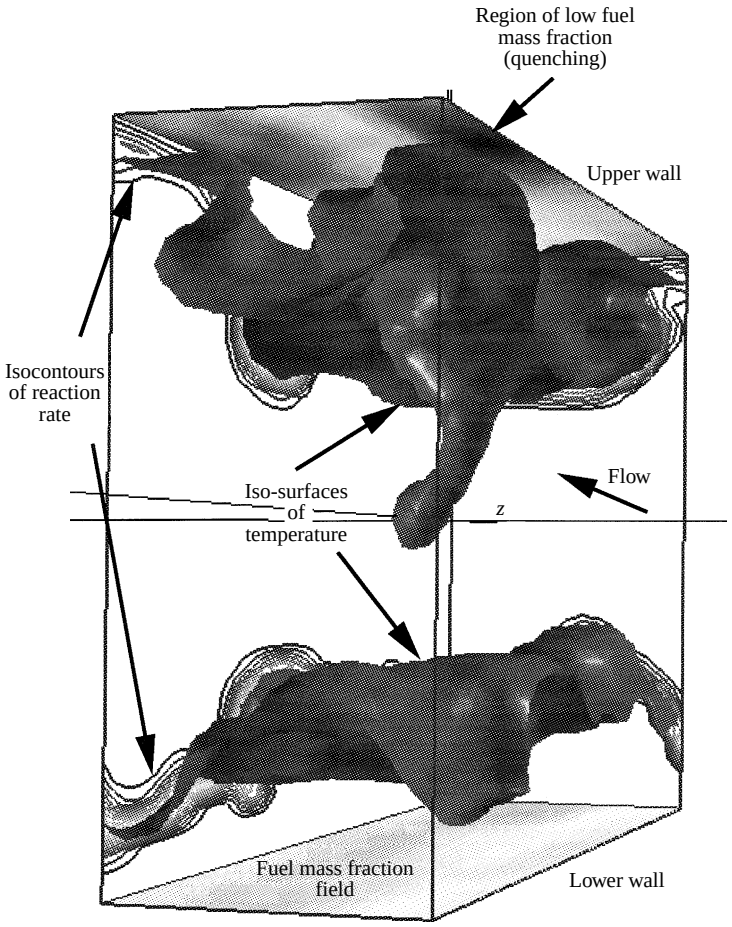

FIGURE 2. Example of DNS of flame–wall interaction result. Two flames (visualized by isosurfaces of temperature) are initiated in the centre of the channel and propagate towards the walls.

in figure 2. This picture shows how the two flame sheets are convoluted by the turbulence and finally interact with the walls, leading to localized quenching and large heat fluxes to the walls. Our objective here is to understand the phenomena for modelling purposes; this requires access to average quantities. To obtain sufficient sampling we performed averages in planes parallel to the walls but also phase averages on different realizations of the flow. This was done by extending the database for turbulent premixed flame–wall interaction (Bruneaux *et al.* 1996): case 1 was repeated 30 times with different initial flow fields obtained by running the channel flow code without combustion; they are separated by ten eddy turn-over times and are statistically independent. The y-direction is normal to the wall and the walls are located at $y = 0$ and $y = 2h$. The periodicity in the x- and z-directions makes the configuration one-dimensional in the mean (but still time dependent). At each instant, averages for all quantitites are performed over the 30 different realizations and in planes parallel to the wall, since the directions x and z parallel to the wall are periodic.

In the DNS, the dynamic viscosity is constant $\mu = \mu_1$; the Reynolds number based on friction velocity u_τ^0 and half-channel width h, $Re_\tau = \rho_1^0 u_\tau^0 h/\mu_1$, is 180; the thermal diffusivity λ varies linearly with temperature: $\lambda = \lambda_1 \left(T/T_1\right)$; the molecular diffusivity

D is related to λ by $D = \lambda/(\rho_1^0 c_p Le)$ where the Lewis number Le is unity. The fresh gas temperature is T_1 and the adiabatic flame temperature is T_2. Thermochemical parameters are such that the temperature factor $\alpha = (T_2 - T_1)/T_2$ is 0.75 and the reduced activation energy $\beta = \alpha T_a/T_2$ is 6. The pre-exponential constant B is chosen so that the unstrained laminar flame speed s_l^0 is given by $s_l^0/u_\tau = 0.363$. The flame thickness δ_l^0 (defined by $\delta_l^0 = (T_2 - T_1)/(\partial T/\partial n)_{max}$) is such that $\delta_l^0/h = 0.15$. More details may be found in Bruneaux *et al.* (1995).

In general, there is no clear scale separation between the quenching zone and viscous zone (the quenching zone is the zone between the wall and the nearest position of the flame during the interaction, and the viscous zone is the near-wall zone where the flow can be considered as purely laminar (Kim, Moin & Moser 1987). Expressed in wall units, the quenching distance is $d^+ = du_\tau/\nu = (1/Pr)(u_\tau/s_l^0)$ after using the definition of the flame reference length d. For most practical hydrocarbon turbulent flames, u_τ will range from 0.1 to 2 $\mathrm{m\,s^{-1}}$ while s_l^0 varies between 0.1 to 1 $\mathrm{m\,s^{-1}}$ so that we do not expect d^+ to be smaller than 0.1 or larger than 2. This means that the quenching zone thickness will be of the order of the viscous sublayer thickness: typically quenching will not happen in the fully turbulent zone (far from the walls) or in the nearly laminar zone (close to the wall). In this particular DNS, the quenching distance is $\delta_Q^+ \simeq 10$, so that the quenching zone thickness is of the order of the viscous sublayer thickness.

2.2. *Exploitation*

All terms of the interface surface density equation (2) can be obtained from the DNS database. The interface between fresh and burnt gases is defined as the isosurface of reduced temperature $\theta = (T - T_1)/(T_2 - T_1) = c_p(T - T_1)/(Y_1^0 \Delta H) = 0.85$ (ΔH is the heat of reaction per unit mass of fuel). This temperature is chosen to match the location of the maximum of the reaction rate $\dot{\omega}_R$ during a laminar flame–wall interaction. The normal to the interface is then calculated as $\boldsymbol{n} = -\nabla\theta/\mid\nabla\theta\mid$. $\boldsymbol{n}$ points towards the fresh gases.

The propagation speed of that surface is obtained using (Trouvé & Poinsot 1994)

$$\omega = \frac{1}{\nabla\theta}\frac{\mathrm{D}\theta}{\mathrm{D}t} = \frac{1}{\rho\mid\nabla\theta\mid}\left(\frac{\partial}{\partial x_i}\left(\frac{\lambda}{c_p}\frac{\partial\theta}{\partial x_i}\right) - \dot{\omega}_R\right). \tag{4}$$

Without heat losses and in the absence of strain or curvature effects, this displacement (or propagation) speed ω is equal to the consumption speed s_l (defined by $s_l = 1/(\rho_1^0 Y_1^0)\int \dot{\omega}_R \,\mathrm{d}n$). However, for turbulent flames, s_l and ω may differ by a large amount. Positive curvature will decrease ω relative to s_l, while negative curvature increases it. If the curvature is large enough, ω may even become negative. Moreover, in the vicinity of the wall, both ω and s_l decrease but ω decreases more rapidly and may become negative when the flame retreats from the wall, seeking a region of lower enthalpy loss, while s_l always stays positive (Wichman & Bruneaux 1995).

To obtain the local surface to volume ratio Σ', the flame area is approximated using the angle between the local temperature gradient and a coordinate direction (Rutland 1989). Since periodic boundary conditions are used, averaging may be performed in the two directions parallel to the walls (x and z) at each instant and over the 30 realizations at the same instant. This averaging is denoted by an overline or brackets $\langle\,\rangle$. The derivation of the following terms is then straightforward: $\Sigma = \langle\Sigma'\rangle$, $\langle a_T\rangle_S = \langle a_T\Sigma'\rangle/\Sigma$ denotes the surface mean, $\langle\omega k_m\rangle_S = \langle\omega k_m\Sigma'\rangle/\Sigma$. The mean reaction rate $\overline{\dot{\omega}}_R$ is obtained by averaging $\dot{\omega}_R$ in planes parallel to the walls and throughout the 30 realizations, and is a function of the y-coordinate (and time).

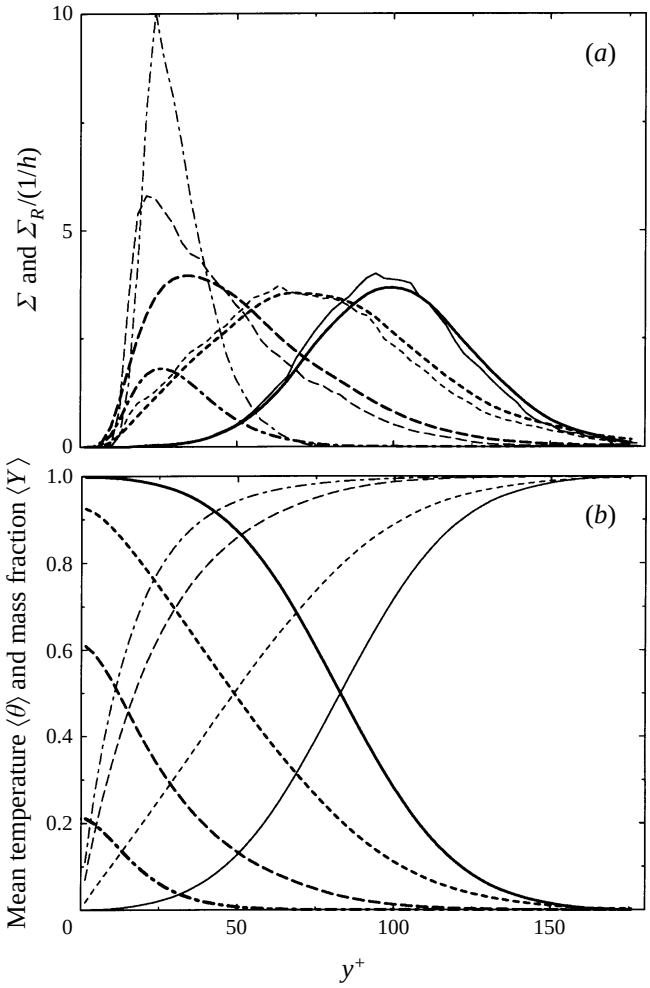

FIGURE 3. Profiles of interface surface density, reactive interface density, mean temperature and mean mass fraction at various times of flame-wall interaction. In (*a*), a thin line corresponds to the interface surface density Σ, and a thick line corresponds to the reactive interface density Σ_R, while in (*b*), a thin line corresponds to the mean temperature $\langle\theta\rangle$, and a thick line corresponds to the mean mass fraction $\langle Y\rangle$: ———, $t/t_f = 3.6$; – – – –, $t/t_f = 7.3$; — — —, $t/t_f = 10.8$; — · —, $t/t_f = 14.6$.

3. Budget of the interface surface density equation

3.1. *Evolution of the flame surface density fields*

It is convenient to replace the mean reaction rate $\overline{\dot{\omega}}_R$ by an equivalent reactive flame surface density Σ_R defined by $\Sigma_R = \overline{\dot{\omega}}_R/(\rho_1^0 Y_1^0 s_l^0)$. In the absence of quenching or strain, Σ is related to $\overline{\dot{\omega}}_R$ by $\overline{\dot{\omega}}_R = \rho_1^0 Y_1^0 s_l^0 \Sigma$ or $\Sigma_R = \Sigma$ since we used Lewis number unity. During the interaction, near the wall, part of this interface is quenched so that $\overline{\dot{\omega}}_R < \rho_1^0 Y_1^0 s_l^0 \Sigma$ and $\Sigma_R < \Sigma$.

Profiles of Σ, Σ_R, $\langle\theta\rangle$, and $\langle Y\rangle$ are presented in figure 3 for various times t normalized by the flame time $t_f = d/s_l^0$. Y is the reduced fuel mass fraction defined by $Y = Y_F/Y_1^0$. Early in the simulation ($t/t_f = 3.6$), the flame is far from the wall, no quenching takes place, and the profile of the interface density Σ matches the profile

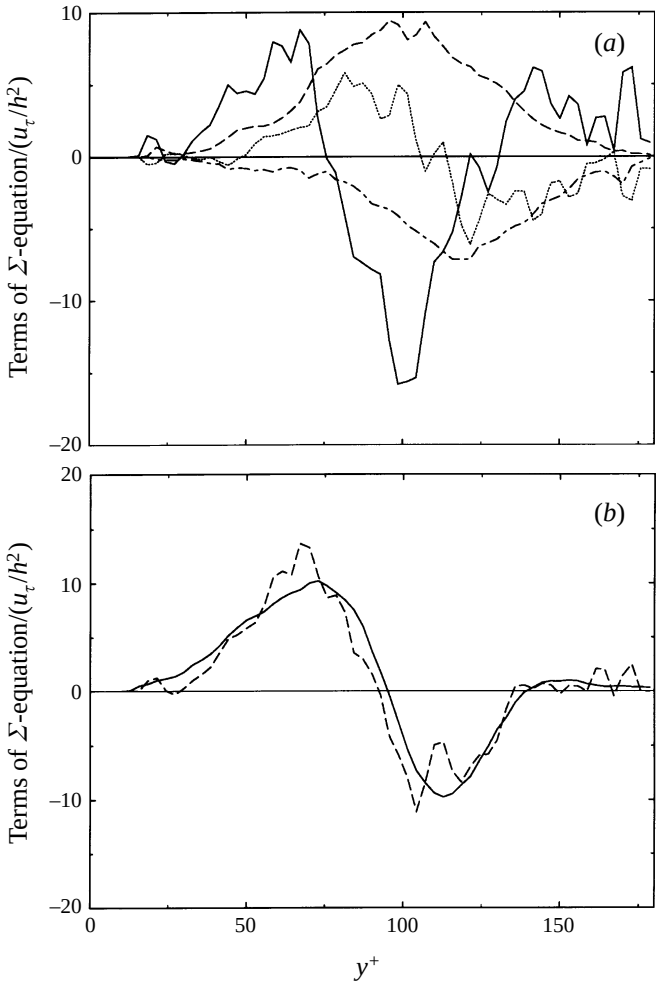

FIGURE 4. Profiles of the terms of the flame surface density equation at time $t/t_f = 3.6$. (*a*) ———, $-(\partial/\partial y)\langle v'\rangle_S \Sigma$ (turbulent diffusion); ·····, $-(\partial/\partial y)\langle \omega n_y\rangle_S \Sigma$ (propagation); — — —, $\langle a_T\rangle_S \Sigma$ (strain); — · —, $2\langle \omega k_m\rangle_S \Sigma$ (destruction). (*b*) ———, $\partial\Sigma/\partial t$ (time variation (left-hand-side term)); — — —, $-(\partial/\partial y)\langle v'\rangle_S \Sigma - (\partial/\partial y)\langle \omega n_y\rangle_S \Sigma + \langle a_T\rangle_S \Sigma + 2\langle \omega k_m\rangle_S \Sigma$ (right-hand-side term)

of the normalized reaction rate Σ_R. The mean fuel mass fraction at the wall is still the initial value and the burnt gases occupy only a small fraction of the channel. Then, at $t/t_f = 7.3$, the flame brush approaches the wall, the temperature gradient near the wall increases while the fuel mass fraction near the wall decreases. No quenching occurs yet and Σ_R still matches Σ.

Later, at $t/t_f = 10.8$, the flame brush starts to interact with the wall and quenching takes place. This decreases the reactive interface density Σ_R relative to the total interface density Σ. The mean temperature gradient is non-zero at the wall, indicating that the mean wall heat flux is no longer zero. Finally at $t/t_f = 14.7$, most of the fresh gases in the channel have been consumed and the interface density is much larger than the reactive surface density. Most of the interface is quenched. Very little fuel is available and the mean wall heat flux is large.

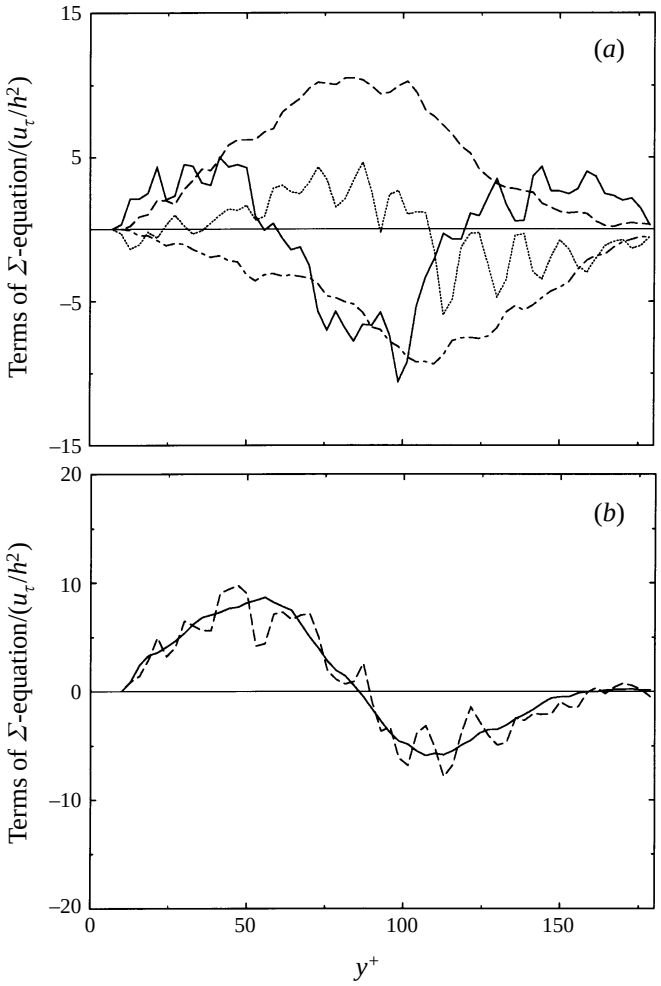

FIGURE 5. As figure 4 but at time $t/t_f = 5.5$.

3.2. *Terms of the Σ-equation*

Using the channel flow simplification (dependence only on y, $\overline{v} = \overline{w} = 0$), the exact interface density equation (2) reduces to

$$\frac{\partial \Sigma}{\partial t} = -\frac{\partial}{\partial y}\langle v' \rangle_S \Sigma - \frac{\partial}{\partial y}\langle \omega n_y \rangle_S \Sigma + \langle a_T \rangle_S \Sigma + 2\langle \omega k_m \rangle_S \Sigma, \tag{5}$$

where n_y is the y-component of the flame normal, v' is the y-component of the fluctuating velocity (also equal to v since the mean velocity in the y-direction, $\overline{v}$, is zero); $\langle a_T \rangle_S$ is the flame strain defined by $a_T = \nabla \cdot \boldsymbol{v} - \boldsymbol{nn} : \nabla \boldsymbol{v}$ and k_m is the curvature of the front defined by $k_m = \frac{1}{2}\nabla \cdot \boldsymbol{n}$.

All the terms on the right-hand side of this equation may be computed in the DNS database and their profiles (averaged over 30 realizations) at various times are presented in figures 4–10, parts (*a*). Parts (*b*) of those figures compare the transient term $\partial \Sigma / \partial t$ to the sum of the terms on the right-hand side and show that the budget of (5) closes quite well.

The first term on the right-hand side of (5) $(-(\partial/\partial y)\langle v' \rangle_S \Sigma)$ is the turbulent

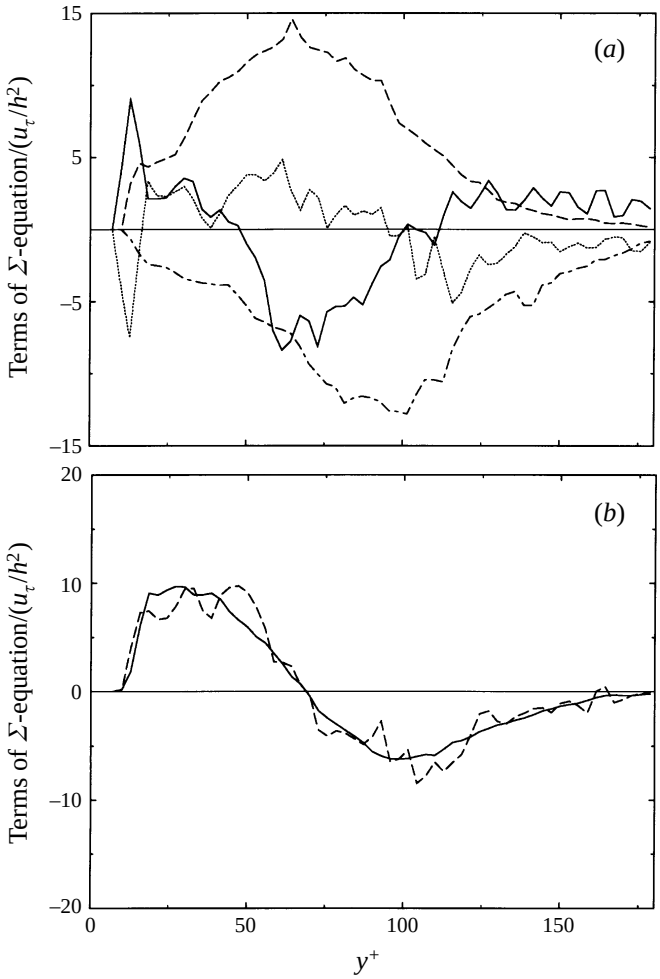

FIGURE 6. As figure 4 but at time $t/t_f = 7.3$.

diffusion of the interface. Its function is to spread the flame since it is negative at the centre of the flame brush, and positive at the edges (gradient diffusion). During the peak of flame–wall interaction ($t/t_f = 9.1, 10.8, 12.8$ and 14.6) it reaches high values due to the large gradients of Σ near the wall. This is a consequence of the flame brush narrowing and flattening due to the geometrical constraints imposed by the wall.

The second right-hand-side term $(-(\partial/\partial y)\langle \omega n_y \rangle_S \Sigma)$ accounts for the propagation of the interface due to its own speed relative to the flow. It contributes to the propagation of the flame towards the wall, since it is positive near the wall and negative far from the wall. This is true except for the very near-wall flame elements where this term is negative, as a result of the negative sign of the propagation speed. Before flame–wall interaction ($t/t_f < 9$), the negative sign of this term is due to the strong curvature at the front of the flame brush. During flame–wall interaction ($t/t_f > 9$) it is due to quenching; the curvature is no longer large, because of the flattening effect of the wall. But flamelet elements that are quenched through enthalpy losses retreat from the wall towards a lower enthalpy loss region (as explained by (Wichman & Bruneaux 1995).

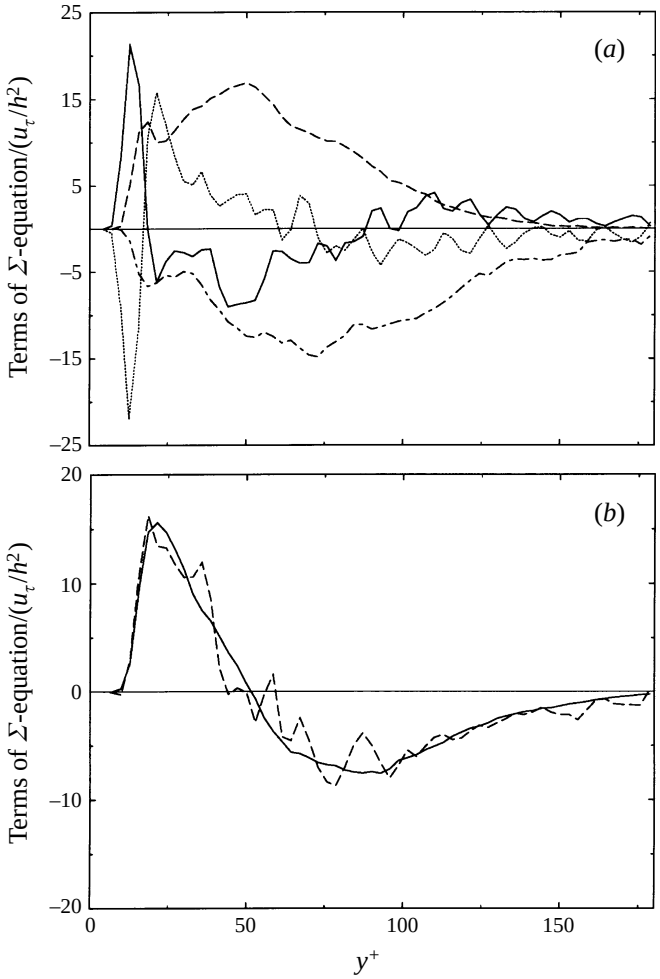

FIGURE 7. As figure 4 but at time $t/t_f = 9.1$.

The third term on the right-hand-side of (5) ($\langle a_T \rangle_S \Sigma$) is the strain of flame elements due to flow divergence. Usually the mean flow and turbulent flow contributions are separated, but here the mean flow contribution is negligible and not shown. The strain term is positive everywhere in the flame brush and at all instants. Therefore it is a production term in the Σ-equation. This result was obtained in previous simulations (Trouvé & Poinsot 1994). It increases during the interaction especially when the flame brush approaches the near-wall region of high turbulence. Late in the interaction ($t/t_f > 10$), highly strained flames are observed in the vicinity of the wall ($y^+ \simeq 20$). Bruneaux *et al.* (1996) showed that horseshoe vortices are responsible for the rapid convection of these strained flame elements towards the wall. Those flamelets come closer to the wall than laminar unstrained flames. There is a near-wall region into which only those highly strained elements penetrate. This mechanism is the source of the existence of peaks of strain rate near the walls as shown in figure 8 or 9.

The fourth right-hand-side term of (5) ($2 \langle \omega k_m \rangle_S \Sigma$) accounts for the combined effect of flame propagation and curvature. It is always negative and acts as a destruction term in the Σ-equation. It remains negative in regions of positive curvature, owing

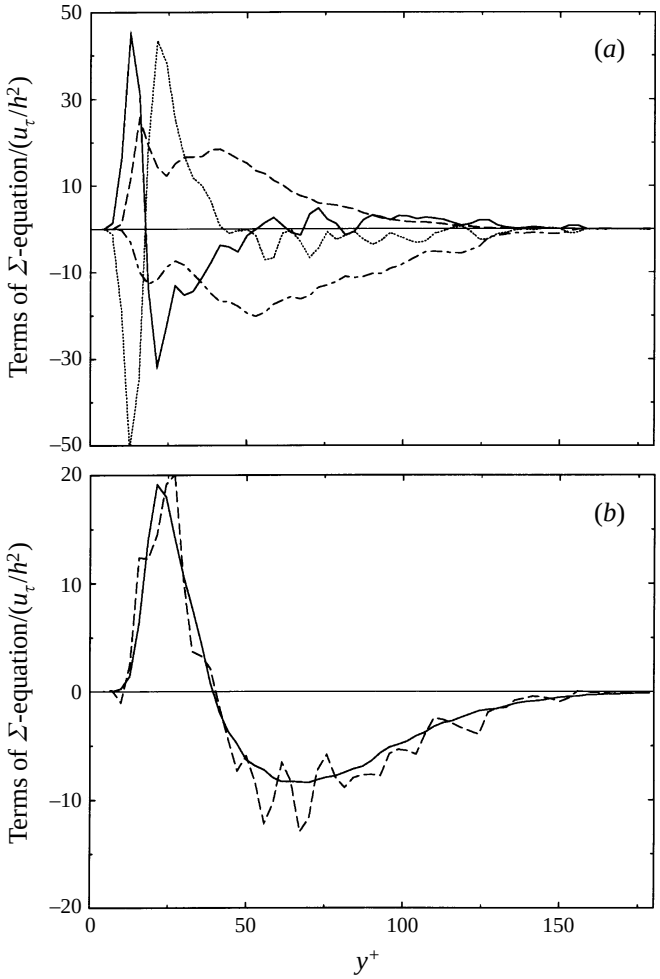

FIGURE 8. As figure 4 but at time $t/t_f = 10.8$.

to the negative displacement speed ω. The negative ω is first due to large positive curvature, and later, it is due to quenching which induces the flame to retreat from the wall. It increases during the interaction.

The order of magnitude of the terms in the Σ-equation changes as the interaction with the wall takes place. First (at $t/t_f = 3.6$) the dominant term is the turbulent diffusion. The strain, curvature and propagation terms are smaller. This is due to the initial condition which corresponds to a planar laminar flame which is strongly diffused by the flow until its wrinkling is compatible with the turbulence. When the flame wrinkling has adapted to the turbulent flow field, but before the interaction with the wall begins (for $4 < t/t_f < 9$), the dominant terms are the turbulent strain and the curvature terms. The propagation term is one quarter of the strain term. (In general, the ratio of the turbulent strain to the propagation term is related to the turbulent–flame speed ratio.) When flame–wall interaction begins, high Σ gradients near the wall appear and induce large values of the propagation and diffusion terms. They dominate until the end of the simulation. In summary, far from the wall, the production (strain) and destruction (curvature) terms are predominant and

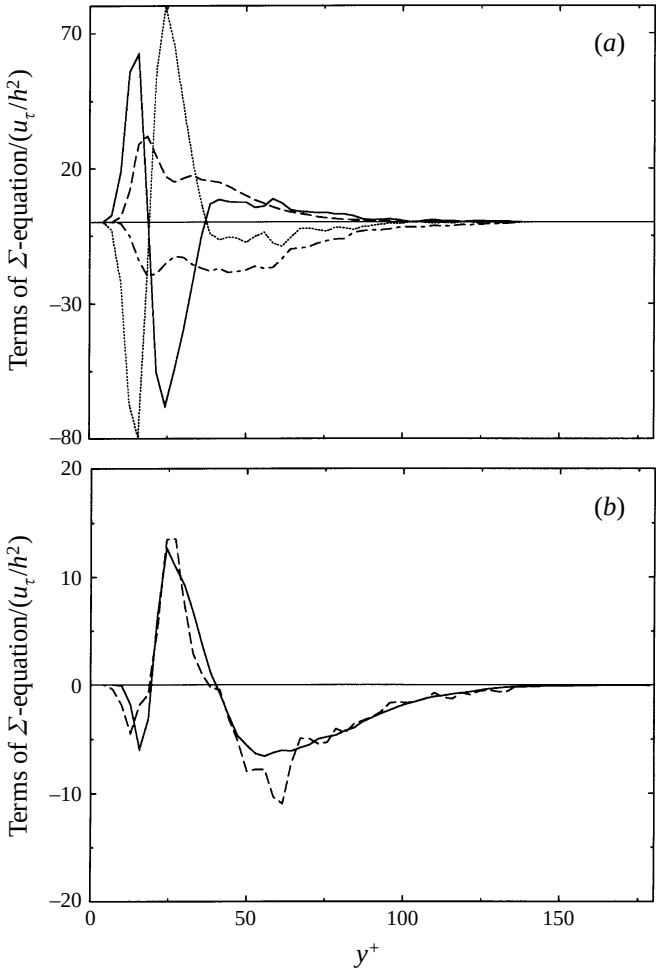

FIGURE 9. As figure 4 but at time $t/t_f = 12.8$.

balanced, the transport (turbulent diffusion and flame propagation) terms are smaller. This balance is reversed during flame–wall interaction due to the large gradients of interface density Σ near the wall.

Figures 4–10 parts (*b*) show that the transient term $\partial\Sigma/\partial t$ balances the sum of the four right-hand-side terms. The budget for the Σ-equation (5) is closed at all times showing that the resolution and sampling used to post-process the database are sufficient. The transient term is obtained using a centred difference with $\Delta t = 1.8t_f$. It shows the initial propagation of the flame towards the wall, and at the end of the interaction, the movement of the flame away from the wall because of quenching and turbulent diffusion ($t/t_f = 12.8$ and 14.6).

4. Modelling flame–wall interaction

We will now study the consequences of wall effects on the modelling of the mean reaction rate in flamelet models. First, we will examine the effect of the wall on flamelet consumption speed $\langle s_l \rangle_S$, which is affected by enthalpy losses to the wall. Then we will study the effect of the wall on flame wrinkling by examining the variation

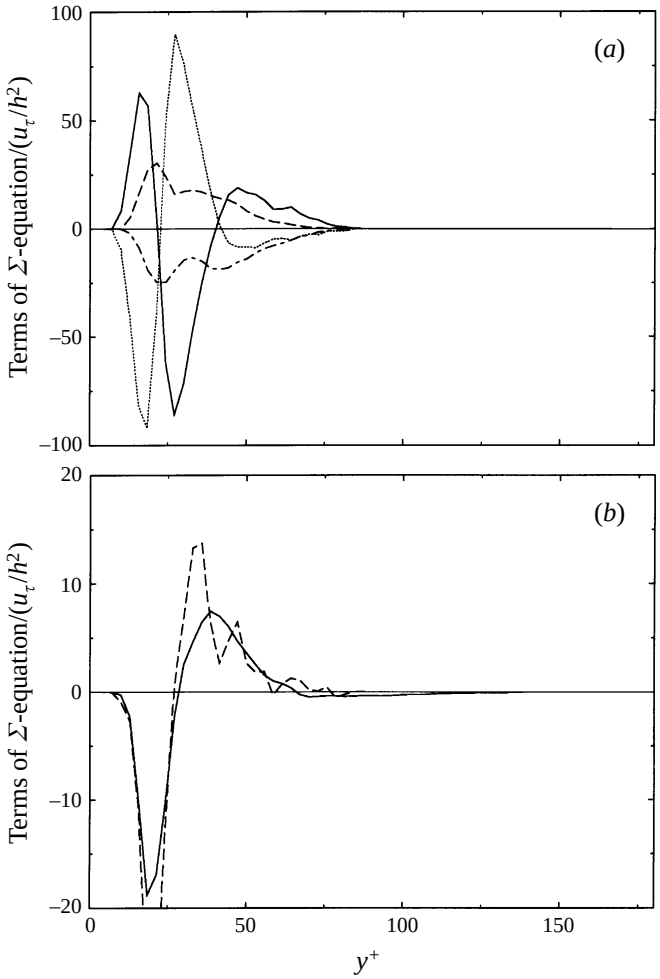

FIGURE 10. As figure 4 but at time $t/t_f = 14.6$.

of Σ through the various terms of the modelled Σ-equation, given by the coherent flame model (CFM).

4.1. *A model for the consumption speed*

It is well-known that interaction between laminar flames and walls or, more generally, the behaviour of non-adiabatic flames may be characterized in terms of the enthalpy loss parameter L_H (Williams 1985; Wichman & Bruneaux 1995), defined by

$$L_H = \frac{H_F^0 - H}{H_F^0 - H_P^0}, \tag{6}$$

where H is the gas enthalpy $H = \sum H_i Y_i$, H_i is the enthalpy of species i, Y_i is the mass fraction of species i, H_F^0 is the fuel enthalpy at the temperature of the fresh gases, and H_P^0 is the enthalpy of the product in the same state. For simple chemistry with fuel the limiting factor (Williams 1985; Wichman & Bruneaux 1995), this reduces to

$$L_H = 1 - (Y + \theta). \tag{7}$$

In an adiabatic premixed flame with unity Lewis number, L_H is zero everywhere. When the flame is non-adiabatic (as near walls), L_H increases, indicating that quenching is possible. This is also true for turbulent flames.

Analytical calculations of Wichman & Bruneaux (1995) show that for a laminar head-on quenching flame–wall interaction, the flame consumption speed is approximately

$$s_l/s_l^0 = \mathrm{e}^{-\beta L_{Hf}/2}, \tag{8}$$

where $s_l = 1/(\rho_1^0 Y_1^0) \int \dot{\omega}_R \, \mathrm{d}n$, L_{Hf} is the enthalpy loss at the flame location, and β the reduced activation energy.

This result may be extended to predict the behaviour of individual flamelets in a turbulent flame brush as follows. Combining the definition of Σ_R, $\overline{\dot{\omega}}_R = \rho_1^0 Y_1^0 s_l^0 \Sigma_R$ with (1), we obtain $\langle s_l \rangle_S / s_l^0 = \Sigma_R/\Sigma$. This ratio will be called the unquenched factor $Q = \langle s_l \rangle_S / s_l^0 = \Sigma_R/\Sigma$. It accounts for the quenching of a turbulent flame. It is 1 if all flamelets elements are burning at speed s_l^0, and decreases when flamelets are quenched. Assuming that the local behaviour of each turbulent flamelet is similar to a laminar interaction:

$$Q = \left\langle \frac{s_l}{s_l^0} \right\rangle_S \tag{9}$$

so that (8) leads to a simple model for Q:

$$Q_{model} = \mathrm{e}^{-\gamma_Q \beta \overline{L}_H}, \tag{10}$$

where γ_Q is a model constant. The best fit with DNS results was obtained for $\gamma_Q = 2$. We recall here that $\overline{L}_H$ is the ensemble-averaged enthalpy loss with a dependence only on y.

Consequently, (1) is modelled as

$$\overline{\dot{\omega}}_R = \rho_1^0 Y_1^0 Q_{model} s_l^0 \Sigma = \rho_1^0 Y_1^0 \, \mathrm{e}^{-\gamma_Q \beta \overline{L}_H} s_l^0 \Sigma. \tag{11}$$

Figure 11 shows the time evolution of global quantities related to the reaction rate. They are obtained through integration over the whole simulation domain. The normalized total reaction rate is displayed along with the total fresh–burnt gas interface. At the beginning, those quantities are almost equal, the interface is burning everywhere (no quenching) and its area increases with flame wrinkling. Then for $t/t_f > 9$ the total reaction rate decreases while the total interface decreases but remains larger than its initial value. The decrease is due to a reduction in flame wrinkling induced by the wall and because more of the interface is quenched. The model for the normalized reaction rate (11) is also displayed and compares well with the DNS value. The decrease relative to the total interface is well predicted. Figure 12 displays profiles that show that the mean reaction rate compares well with the model at all times.

4.2. *Terms of the interface surface density equation*

The model given above provides a good estimate of the mean reaction rate if the interface surface density Σ is known. We now focus our work on the determination of Σ. One method is to construct a conservation equation for this quantity based on heuristic considerations as done by many authors (Cant *et al.* 1990; Candel *et al.* 1990; Boudier *et al.* 1992). Another is to model each individual term of the exact Σ-equation (2) or a related equation (Mantel & Borghi 1994; Trouvé & Poinsot 1994). We choose to start from heuristic equations but to validate each term in these model equations by comparison with the exact terms in (2).

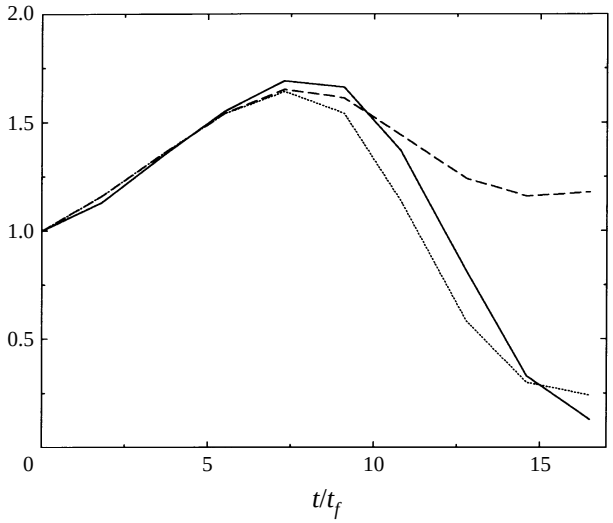

FIGURE 11. Evolution of the total reduced reaction rate and comparison with the model. The difference between the total equivalent reactive flame surface, $(1/h)\int \Sigma_R \mathrm{d}y$, and the total interface, $(1/h)\int \Sigma \mathrm{d}y$, show the effect of quenching. ———, Total equivalent reactive flame surface, $(1/h)\int \Sigma_R \mathrm{d}y = 1/(\rho_1^0 Y_1^0 s_l^0 h)\int \overline{\dot{\omega}}_R \mathrm{d}y$; — — —, Total interface, $(1/h)\int \Sigma \mathrm{d}y$; ·····, model for total equivalent reactive flame surface, $(1/h)\int Q_{model}\Sigma \mathrm{d}y$.

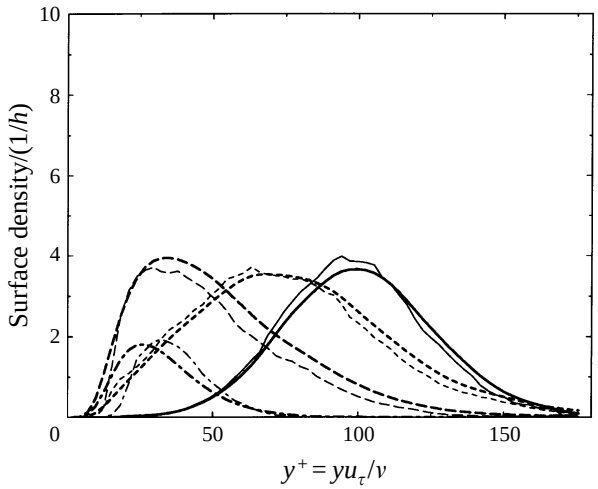

FIGURE 12. Profiles of reactive surface density, and test of the model for quenched ratio, at four different times: ———, $t/t_f = 3.6$; - - - -, $t/t_f = 7.3$; — — —, $t/t_f = 10.8$; —·—, $t/t_f = 14.6$; ———, reactive flame surface density Σ_R (measured in DNS); ———, $Q_{model}\Sigma$ where Σ is measured in DNS and Q_{model} is given by the model.

All modelling methods lead to the same form for the conservation equation of Σ. As an example, the CFM (Candel *et al.* 1990; Boudier *et al.* 1992) can be written (for a one-dimensional turbulent flame propagating in the y-direction)

$$\frac{\partial \Sigma}{\partial t} = \frac{\partial}{\partial y}\left(\frac{\nu_t}{\sigma_\Sigma}\frac{\partial \Sigma}{\partial y}\right) + \alpha_m K_t \Sigma - \beta_m D_\Sigma \Sigma, \tag{12}$$

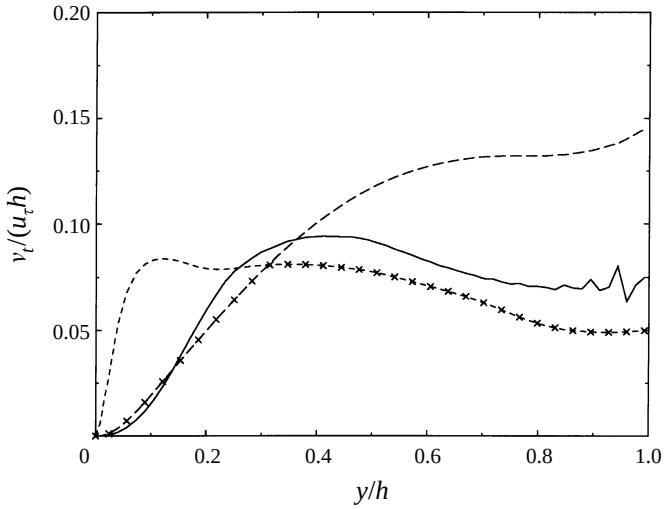

FIGURE 13. Profiles of turbulent viscosity v_t: ———, calculated with the DNS code $v_t = -\langle u'v'\rangle/(d\bar{u}/dy)$; – – – –, $v_t^\infty = c_\mu k^2/\epsilon$; — — —, using a Van Driest mixing length, $v_t^0 = c_\mu^1\left(\kappa y\left(1-\mathrm{e}^{-y^+/A^+}\right)\right)k^{1/2}$; ×, modelled turbulent viscosity corrected in the log zone, $\min\left(v_t^\infty, v_t^0\right)$.

where $(\partial/\partial y)(v_t/\sigma_\Sigma)(\partial\Sigma/\partial y)$ is the modelled turbulent diffusion term; v_t is the turbulent viscosity; σ_Σ is a turbulent Schmidt number ($\sigma_\Sigma = 1$); K_t is the turbulent strain rate; $\beta_m D_\Sigma \Sigma$ is the destruction term which contains the annihilation rate D_Σ; α_m and β_m are model constants ($\alpha_m = 2.1$, $\beta_m = 1$). The two last terms on the right-hand side are, respectively, the proposed closures for the strain $\langle a_T\rangle_S \Sigma$ and curvature $\langle \omega k_m\rangle_S \Sigma$ terms.

In the following sections, we will model the effect of the wall on each term of (12).

4.2.1. *Turbulent diffusion term*

Turbulent diffusion accounts for the transport of flame surface by turbulent convection; it is modelled via a turbulent viscosity v_t. Despite the fact that theoretical work (Bray *et al.* 1981) as well as recent DNS of variable-density flames (Trouvé *et al.* 1994; Rutland & Cant 1994) show that counter-gradient diffusion of species and surface density are found in low-turbulence intensity flames, the gradient diffusion assumption remains widely used. We will see that it is a good approximation here (as expected since counter-gradient diffusion mechanisms are driven by density changes).

The usual expression for v_t far from the wall is (Launder & Spalding 1972)

$$v_t^\infty = c_\mu k^2/\epsilon, \tag{13}$$

where $c_\mu = 0.09$, k is the turbulent kinetic energy, and ϵ the turbulent dissipation.

Figure 13 shows the exact v_t (calculated from the DNS), compared with (13). In the log region (which stretches up to $h/3$ in this calculation), expression (13) overestimates the turbulent viscosity. It is therefore necessary to correct the expression for v_t in the log zone. We choose to use the Van Driest mixing length (Launder & Spalding 1972) which gives

$$v_t^0 = c_\mu^1\left(\kappa y\left(1-\mathrm{e}^{-y^+/A^+}\right)\right)k^{1/2}, \tag{14}$$

where $c_\mu^1 = 0.50$, $\kappa = 0.41$, $y^+ = yu_\tau/v$ and $A^+ = 26$.

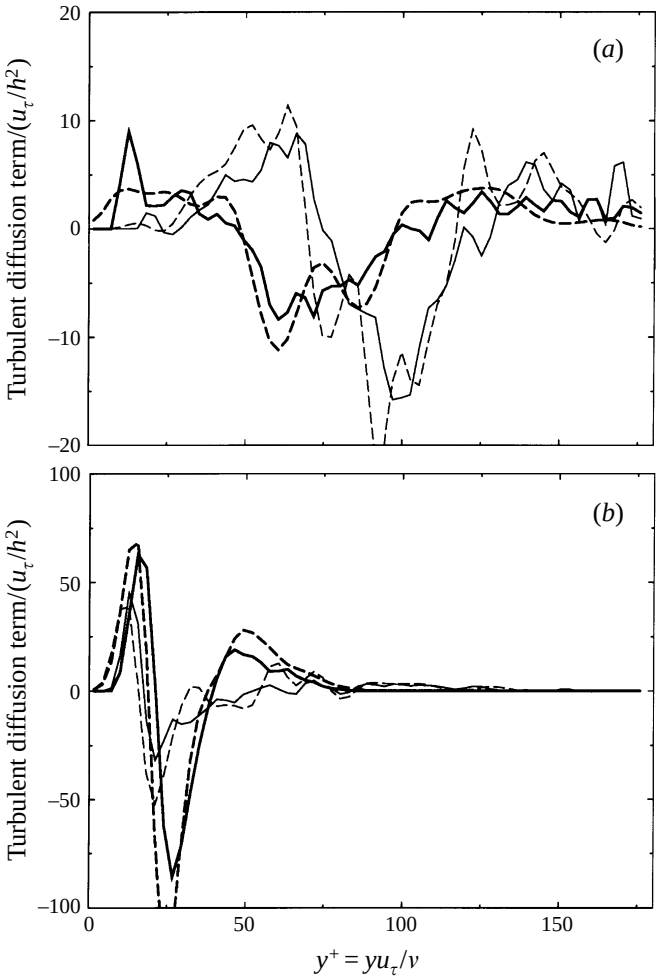

FIGURE 14. Turbulent diffusion term at four times of flame–wall interaction. (*a*) ———, $t/t_f = 3.6$; ———, $t/t_f = 7.3$; (*b*) ———, $t/t_f = 10.8$; ———, $t/t_f = 14.6$. Comparison between model and DNS: ———, DNS result $-(\partial/\partial y)\left(\langle v'\rangle_S \Sigma\right)$; — — —, modelled term $(\partial/\partial y)\left((\nu_t/\sigma_\Sigma)(\partial\Sigma)/(\partial y)\right)$.

A proper expression for the turbulent viscosity is therefore $\nu_t = \min\left(\nu_t^\infty, \nu_t^0\right)$, as shown in figure 13.

Figure 14 shows the comparison between the modelled diffusion term using this turbulent viscosity, and the DNS turbulent diffusion term. The modelled term agrees very well with the DNS results. This expression will be used in the rest of this paper.

4.2.2. *Strain term*

The strain term (the second term on the right-hand side of (2)) accounts for straining of flame elements by turbulence. In many recent flamelet models, the strain term is estimated using the Intermittent Turbulent Net Flame Stretch (ITNFS) model (Meneveau & Poinsot 1991; Boudier *et al.* 1992):

$$K_t = \frac{\epsilon}{k} f\left(\frac{u''}{s_l^0}, \frac{L}{\delta_l^0}\right), \tag{15}$$

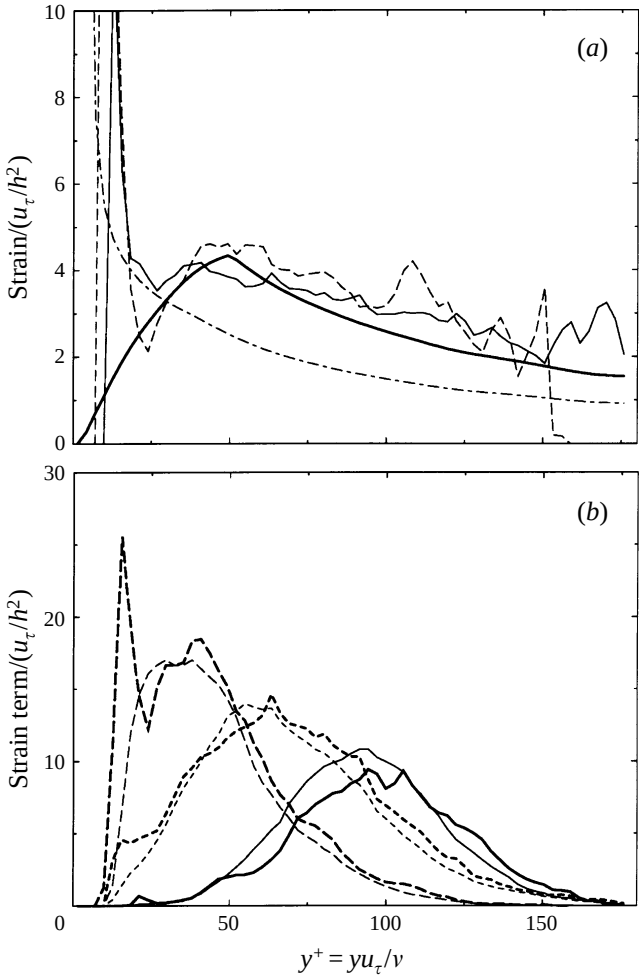

FIGURE 15. Profiles of strain term. (*a*) The profiles of the exact strain term $\langle a_T \rangle_S$ computed by the DNS at (———), $t/t_f = 7.3$ and (— — —), $t/t_f = 10.8$; the profile of the modelled term using the new model: (———), $\alpha_m K_t$, and the profile using a simpler model often used in CFD codes to compute CFD codes to compute flame–wall interactions (— · —), ϵ/k. (*b*) The DNS term $\langle a_T \rangle_S \Sigma$ (with a thin line) is compared to the new model $\alpha_m K_t \Sigma$ (with a thick line), at different times of the interaction: ———, $t/t_f = 3.6$; - - - - , $t/t_f = 7.3$; — — —, $t/t_f = 10.8$.

where $u'' = (2k/3)^{1/2}$ is the RMS turbulent velocity, L the integral length scale in the fresh gases, δ_l^0 is the laminar flame thickness, and f is a function given in the work of Meneveau & Poinsot (1991).

In the fully turbulent region ($y^+ > 50$) we expect the turbulence to strain the flame in accord with (15), with $L = L_0$, the integral scale. In the vicinity of the wall, vortices larger than their distance to the wall are not expected to survive. So the integral scale in the ITNFS model needs to be corrected. If L is equal to its value in the channel L_0 for $y^+ > 50$, it is expected to be approximately proportional to the wall distance for $y^+ < 50$, as is the mixing length (Launder & Spalding 1972). A similar idea was used by Steiner & Boulochos (1995) in their modelling of turbulent flame speed in an engine. We therefore correct the length scale: $L = L_0$ for $y^+ > 50$, and $L = \frac{1}{50} y^+ L_0$ for $y^+ < 50$. Determination of L_0 is difficult in the channel. We do not use the Van

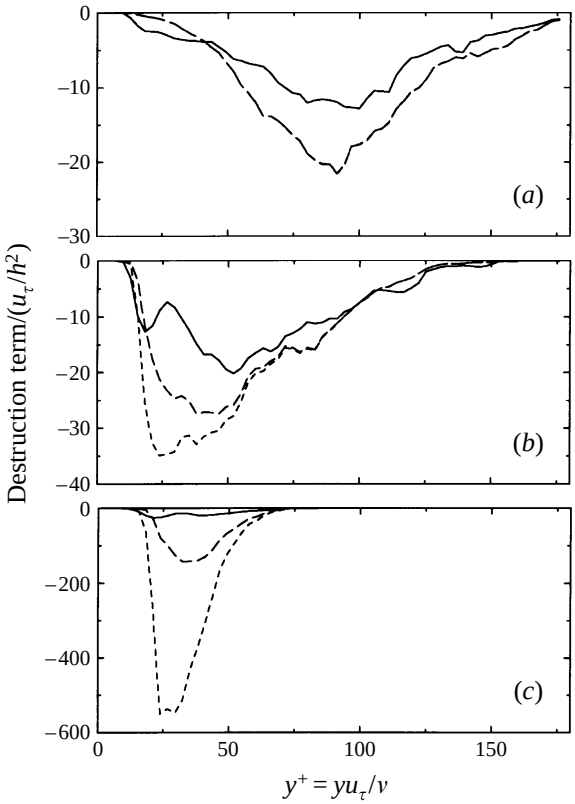

FIGURE 16. Profiles of destruction term, comparison of DNS and model. The expression for a model without quenching is also displayed. (*a*) $t/t_f = 7.3$, (*b*) $t/t_f = 10.8$ and (*c*) $t/t_f = 14.6$, ———, $2\langle \omega k_m \rangle_S \Sigma$ measured in DNS; — — —, $-\beta_m(\rho_1^0 Y_1^0 s_l^0 Q_{model} \Sigma^2)/(\overline{\rho Y_F})$ model with quenching effects, - - - - , $-\beta_m(\rho_1^0 Y_1^0 s_l^0 \Sigma^2)/(\overline{\rho Y_F})$ model without quenching effects. Note that in (*a*), the two model expressions (with and without quenching effects) merge because there is no quenching at this instant.

Driest mixing length, since it is relative to the direction normal to the wall, while the most effective vortices are straining the flame in the streamwise direction. We take (Kim *et al.* 1987) $L_0 = 2h$.

In figure 15 this expression is tested against DNS results for the strain term in (2) and also shows good agreement. Figure 15 also shows the error done when ϵ/k is used for the strain rate (an approximation used in many flamelet models (Duclos, Veynante & Poinsot 1993). The peak of the strain term near the wall in figure 15(*a*) is explained by Bruneaux *et al.* 1996 and due to highly strained flame elements approaching the wall very closely and pushed there by horseshoe vortices. As demonstrated in figure 15(*b*), these events have a small effect on the source term in the Σ-equation ($\langle a_T \rangle_S \Sigma$)) and they may be simply omitted in the model at this stage.

4.2.3. *Destruction term*

As shown in §3.2, the curvature term $\langle \omega k_m \rangle_S \Sigma$ in (2) is a destruction term. It accounts for flame shortening due to flame front interaction. In flamelet models this term is usually modelled as $D_\Sigma \Sigma$ with a model constant β_m. Here, we have to modify this term to account for the wall. To do this, we perform a new derivation of this term.

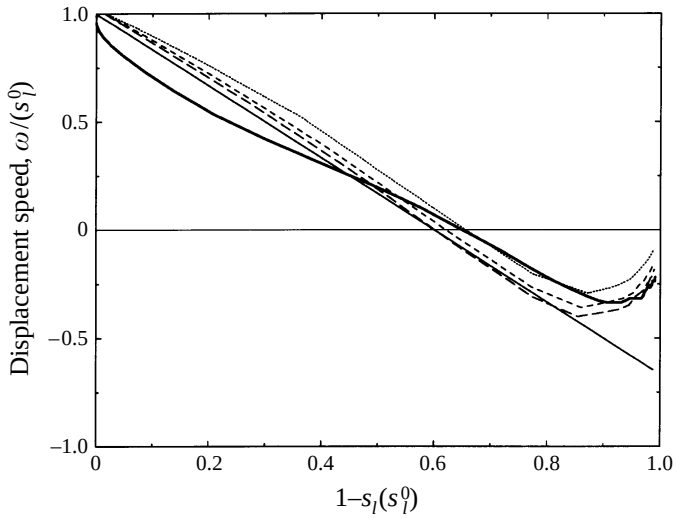

FIGURE 17. Correlation between displacement speed, ω, and laminar flame speed, s_l, for a laminar flame–wall interaction. ———, calculation using the DNS code, with the parameters of table 1; ·····, calculation with a theoretical-numerical approach, $\beta = 4$; – – – –, calculation with a theoretical-numerical approach, $\beta = 6$; — — —, calculation with a theoretical-numerical approach, $\beta = 8$; ———, $1 - \left(1 - s_l/s_l^0\right)/\gamma_{\omega,l}$ with $\gamma_{\omega,l} = 0.6$.

We start by writing the annihilation rate D_Σ as $1/t_c$, where t_c is a characteristic consumption time. This time may be estimated as the ratio of a mass of fuel m_f per unit volume V_T to the volumetric fuel mass consumption rate: $t_c = m_f/(\rho_1^0 Y_1^0 \langle s_l \rangle_S S)$, where S is the flame area in volume V_T ($S = \Sigma V_T$) and $m_f = \overline{\rho Y_F} V_T$. This leads to the following expression for the annihilation rate:

$$D_\Sigma = \frac{\rho_1^0 Y_1^0 \langle s_l \rangle_S \Sigma}{\overline{\rho Y_F}}. \tag{16}$$

Special care has to be taken close to walls, because the consumption speed $\langle s_l \rangle_S$ decreases rapidly there due to quenching (in classical flamelet models $\langle s_l \rangle_S = s_l^0$ is used).

We already have derived and validated a model for $\langle s_l \rangle_S$ (see (10)) : $\langle s_l \rangle_S = Q_{model} s_l^0$, and therefore a destruction term that accounts for wall effects may be written:

$$D_\Sigma = \frac{\rho_1^0 Y_1^0 s_l^0 Q_{model} \Sigma}{\overline{\rho Y_F}}. \tag{17}$$

This expression is compared to the exact destruction term in figure 16 at various times. The modelled expression without the wall correction is also displayed. Before quenching ($t/t_f = 7.3$ and 10.8) the comparison is good, and it is improved by the wall correction. Later ($t/t_f = 14.6$), the modelled term over-estimates the destruction term, but the quenching correction clearly improves the comparison.

4.2.4. *Propagation term*

Usually, the propagation term is not modelled in flamelet models. The ratio of this laminar term to the dominant terms is related to the turbulent–laminar flame speed ratio. Hence, for a highly turbulent freely propagating flame it is neglected. However,

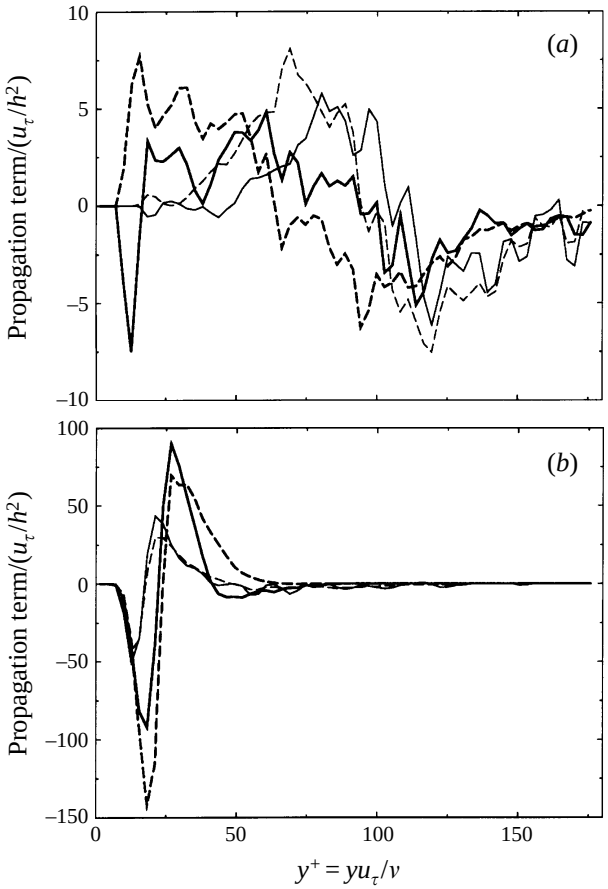

FIGURE 18. Profiles of the propagation term at four times of flame–wall interaction. Comparison of model and DNS. (*a*) ———, $t/t_f = 3.6$; ———, $t/t_f = 7.3$; (*b*) ———, $t/t_f = 10.8$; ———, $t/t_f = 14.6$; ———, DNS result for $-(\partial/\partial y)\langle\omega n_y\rangle_S \Sigma$; — — —, model $(\partial/\partial y)\left(s_l^0\left(1-(1-Q_{model})/\gamma_\omega\right)\Sigma\right)$.

it becomes important near walls as shown above and needs to be modelled in the flame–wall configuration.

Two effects influence the flame displacement speed. First, flame stretch affects the flamelet structure (Candel *et al.* 1990; Cant *et al.* 1990; Bray 1990). Second, near walls, quenching of flamelet elements may cause the displacement speed to become negative, when flamelets retreat from near-wall high-enthalpy-loss regions. At this point, we neglect stretch effects and retain only the effects of quenching.

For a laminar flame–wall interaction (without stretch effects), the flame displacement speed ω is directly linked to the consumption speed s_l (Wichman & Bruneaux 1995). Without quenching, $\omega = s_l = s_l^0$. When flames come closer to the wall, s_l decreases but the displacement speed ω decreases faster. Figure 17 displays ω vs. s_l/s_l^0 for four calculations: a laminar interaction in conditions similar to the turbulent calculation presented here and three calculations using the approach of (Wichman & Bruneaux 1995), where the reduced activation energy β is varied. It appears that consumption and displacement speeds during quenching may be related by

	Mean reaction rate	Evolution equation for Σ			
		Destruction	Propagation	Turbulent diffusion	Strain
Exact expression	$\overline{\dot{\omega}}_R = \rho_1^0 Y_1^0 \langle s_l \rangle_S \Sigma$	$\langle \omega k_m \rangle_S \Sigma$	$-\langle \omega n_y \rangle_S \Sigma$	$-\frac{\partial}{\partial y} \langle v' \rangle_S \Sigma$	$\langle a_T \rangle_S \Sigma$
Initial model	$\overline{\dot{\omega}}_R = \rho_1^0 Y_1^0 s_l^0 \Sigma$	$-\beta_m D_\Sigma \Sigma$ $D_\Sigma = \frac{\rho_1^0 Y_1^0 s_l^0 \Sigma}{\overline{\rho Y_F}}$		$\frac{\partial}{\partial y}\left(\frac{\nu_t}{\sigma_\Sigma}\frac{\partial \Sigma}{\partial y}\right)$ $\nu_t^\infty = c_\mu k^2/\epsilon$	$\alpha_m K_t \Sigma$ $K_t = \frac{\epsilon}{k} f\left(\frac{u''}{s_l^0}, \frac{L}{\delta_l^0}\right)$ $L = L_0$
Wall effect	Quenching through heat losses $Q_m = \mathrm{e}^{-\gamma_Q \beta \overline{L}_H}$			Decrease of turbulence scales in the vicinity of the walls	
New model	$\overline{\dot{\omega}}_R = \rho_1^0 Y_1^0 s_l^0 Q_m \Sigma$	$D_\Sigma = \frac{\rho_1^0 Y_1^0 s_l^0 Q_m \Sigma}{\overline{\rho Y_F}}$	$\frac{\partial}{\partial y}(s_l^0 \Sigma (1 - (1 - Q_m)/\gamma_\omega))$	$\nu_t^0 = c_\mu^1 k^{1/2} \kappa y$ $\left(1 - \mathrm{e}^{-y^+/A^+}\right)$ in log. zone	$L = \frac{y^+}{50} L_0$ if $y^+ < 50$

TABLE 1. Description of the new model with wall effects.

the following expression:

$$\frac{\omega}{s_l^0} \simeq 1 - \left(1 - s_l/s_l^0\right)/\gamma_{\omega,l}, \tag{18}$$

where $\gamma_{\omega,l} = 0.6$.

Neglecting the effects of wrinkling on the propagation term and using the model already derived for the consumption speed, a simple model for the propagation term is then

$$\left(-\frac{\partial}{\partial y}\langle \omega n_y \rangle_S \Sigma\right)_{model} = \frac{\partial}{\partial y}\left(s_l^0 \left(1 - (1 - Q_{model})/\gamma_\omega\right) \Sigma\right), \tag{19}$$

where γ_ω is a model constant. This model is compared to the DNS database in figure 18 for $\gamma_\omega = 0.3$. It describes the global propagation of the flame brush towards the wall and the retreat due to negative values of ω. In order to explain the difference between $\gamma_{\omega,l}$ and γ_ω, we calculated $\gamma_{\omega,l}$ for the laminar calculations in a stagnation line flow, performed in the work of Bruneaux *et al.* (1996). We found that $\gamma_{\omega,l}$ is reduced down to $\gamma_{\omega,l} \simeq 0.3$ for strain rates equivalent to those found in the turbulent simulation.

4.3. *Budget for the modelled interface surface density equation*

Table 1 presents the terms of the present model of the Σ-equation as well as differences with the classical coherent flame model without the flame–wall interaction submodel. It is important to note the differences from the FIST model (Poinsot *et al.* 1993). The latter is a type of 'law-of-the-wall' model in which $y^+ < 150$ is not resolved but modelled through an *ad-hoc* relation. Here, our analysis of the terms of the exact

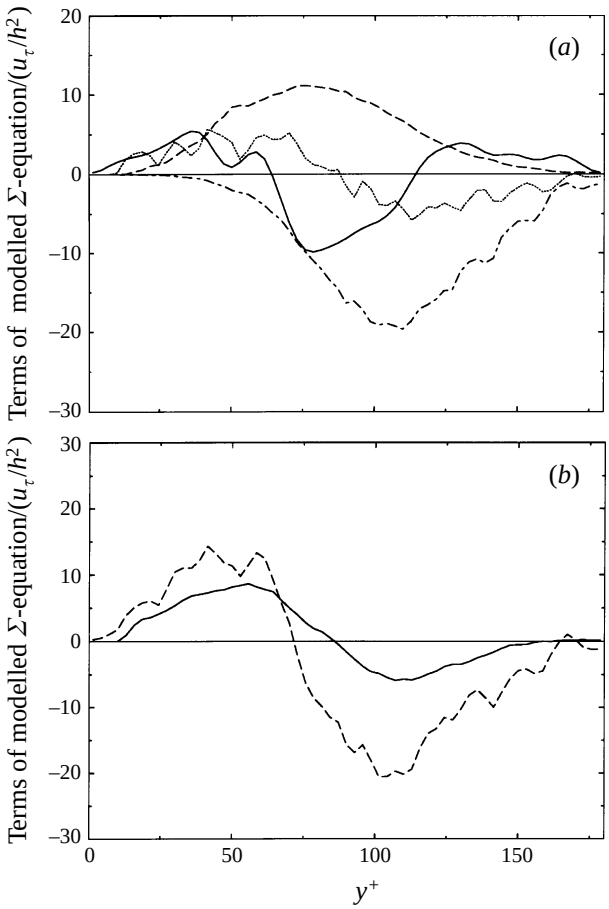

FIGURE 19. Profiles of the terms of the modelled flame surface density equation and budget, at time $t/t_f = 5.5$. (*a*) ———, $(\partial/\partial y)\left((\nu_t/\sigma_\Sigma)/(\partial\Sigma/\partial y)\right)$; ·····, $(\partial/\partial y)\left(s_l^0\left(1-(1-Q_{model})/\gamma_\omega\right)\Sigma\right)$; — — —, $\alpha_m K_t \Sigma$; — · —, $-\beta_m(\rho_1^0 Y_1^0 s_l^0 Q_{model}\Sigma^2)/(\overline{\rho Y_F})$; (*b*) ———, $(\partial\Sigma/\partial t)$; — — —, $(\partial/\partial y)\left((\nu_t\sigma_\Sigma)/(\partial\Sigma\partial y)\right)+(\partial/\partial y)\left(s_l^0\left(1-(1-Q_{model})/\gamma_\omega\right)\Sigma\right)+\alpha_m K_t\Sigma-\beta_m(\rho_1^0 Y_1^0 s_l^0 Q_{model}\Sigma^2)/(\overline{\rho Y_F})$.

equation for the interface surface density allows us to model wall effects on flame propagation into the near-wall region.

A budget for the wall-corrected modelled Σ-equation is presented for the first instants of interaction in figures 19, 20. Profiles of the modelled right-hand-side terms are presented. The second part of those figures compares the transient term $\partial\Sigma/\partial t$ obtained from the DNS, with the sum of the modelled right-hand-side terms. They compare quite well for the first instants of interaction ($t/t_f < 10$). It shows that the model with wall correction is approximately able to account for the change in Σ. At late interaction times, the comparison is not as good, but remains satisfactory as shown in the next section.

4.4. *Final flamelet model with flame–wall correction terms*

In the previous sections, we have derived closures for all terms of the flame surface density conservation equation. These closures include wall corrections. The final set of equations is a flamelet model which should be valid both far from and close to the walls. In this section, we test this model in the configuration used for the DNS and

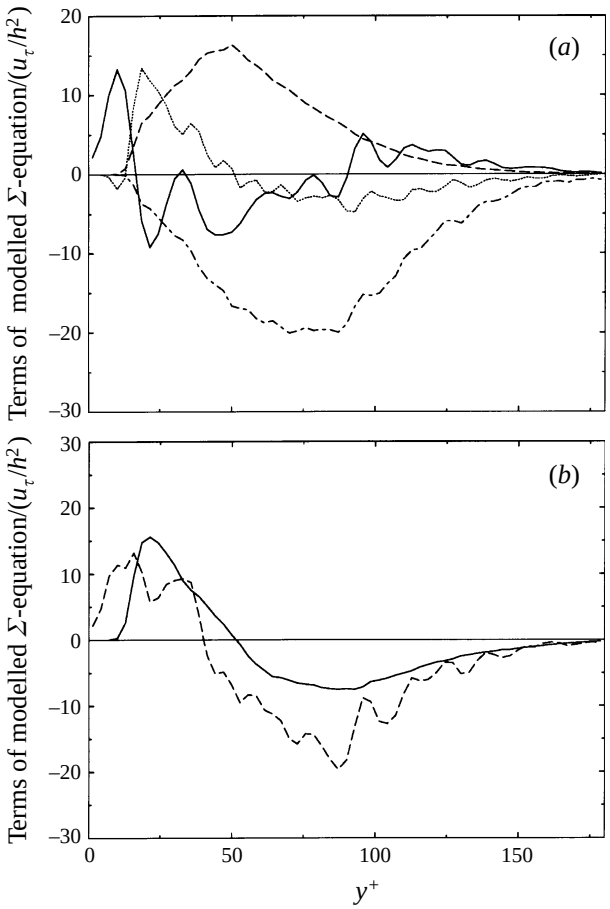

FIGURE 20. As figure 19 but at time $t/t_f = 9.1$.

compare results provided by the model and by the DNS in terms of total reaction rate, mean fuel mass fraction in the channel, heat flux at the wall and fuel mass fraction at the wall.

In the case of propagating turbulent flames in a channel flow, flamelet model calculation reduce to a one-dimensional simulation where variables (the mean temperature $\overline{T}$, the flame surface density Σ and the mean fuel mass fraction $\overline{Y_F}$) are functions of the wall distance y and of time t only. Since the flow has constant density and is not influenced by the flame, no momentum equation is required. A classical eddy diffusivity is used for turbulent transport and for heat transfer (Kays & Crawford 1993; Launder & Spalding 1972) and the flame surface density closure derived in the previous sections is used for the mean reaction term:

$$\left.\begin{aligned}
\frac{\partial \rho c_p \overline{T}}{\partial t} &= \frac{\partial}{\partial y}\left[\left(\bar{\lambda} + \rho c_p \frac{\nu_t}{Pr_t}\right)\frac{\partial \overline{T}}{\partial y}\right] + c_p\left(T_2 - T_1\right)\rho_1^0 Y_1^0 s_l^0 Q\Sigma, \\
\frac{\partial \rho \overline{Y_F}}{\partial t} &= \frac{\partial}{\partial y}\left[\left(\rho \overline{D} + \rho \frac{\nu_t}{LePr_t}\right)\frac{\partial \overline{Y_F}}{\partial y}\right] + \rho_1^0 Y_1^0 s_l^0 Q\Sigma, \\
\frac{\partial \Sigma}{\partial t} &= \frac{\partial}{\partial y}\left(\frac{\nu_t}{\sigma_\Sigma}\frac{\partial \Sigma}{\partial y}\right) + \frac{\partial}{\partial y}\left(s_l^0\left(1-(1-Q)/\gamma_\omega\right)\Sigma\right) + \alpha_m K_t \Sigma - \beta_m D_\Sigma \Sigma,
\end{aligned}\right\} \quad (20)$$

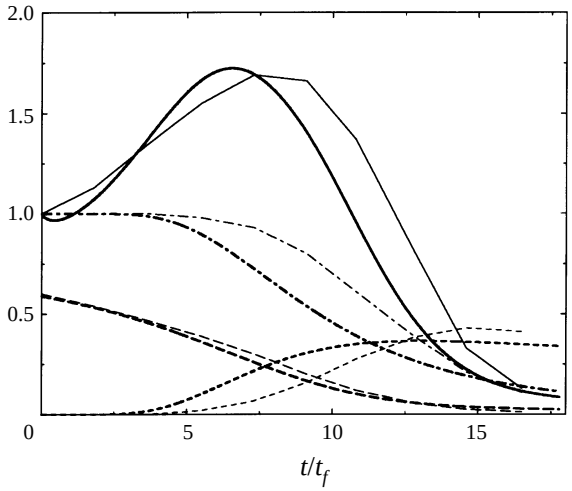

FIGURE 21. Results of the one-dimensional model and comparison with DNS. A thin line correspond to DNS results, a thick line corresponds to the one-dimensional model with wall corrections: ———, total reaction rate $\int \Sigma Q \mathrm{d}y$; – – – –, mean wall heat flux $|-\lambda(\partial\overline{T}/\partial y)(0,t)|/(\rho_1^0 s_l^0 c_p(T_2-T_1))$; — — —, total mean mass fraction $(1/h)\int \overline{Y_F}(y,t)/Y_1^0 \mathrm{d}y$; —·—, mean wall mass fraction $\overline{Y_F}(0,t)/Y_1^0$.

where Pr_t is the turbulent prandtl number ($Pr_t = 0.85$ (Kays & Crawford 1993); $Le = \lambda/(\rho c_p D) = 1$ is the Lewis number; K_t and D_Σ are the wall-corrected strain and annihilation factors ((15) and (17)). The turbulent diffusivity ν_t is calculated from (13) corrected with (14) in the log zone.

In the absence of walls, Q is equal to unity everywhere and the previous system is equivalent to the classical CFM (Candel *et al.* 1990; Duclos *et al.* 1993) (except for the propagation term $(\partial/\partial y)\left(s_l^0\Sigma\right)$ which has been added here). In the presence of walls, the model for Q derived above is used:

$$Q = \mathrm{e}^{-\gamma_Q \beta \overline{L_H}} \quad \text{and} \quad \overline{L_H} = 1 - \frac{\overline{T}-T_1}{T_2-T_1} - \frac{\overline{Y_F}}{Y_1^0}. \tag{21}$$

This model for Q appears explicitly in (20) but also in the expressions for D_Σ and the mean reaction rate.

Equation 20 is solved using a centred finite-difference scheme and explicit time integration. The configuration corresponds to a one-dimensional calculation of the half-channel. The wall is located at $y = 0$, and the calculation domain extends to the middle of the channel $y = h$. One-dimensional meshes of 16, 32 and 64 points have been tried and the model results proved to be grid insensitive.

Initial conditions raise a specific difficulty because the DNS was initialized with a laminar flame, a difficult condition for a flamelet model. The $\overline{T}$- and $\overline{Y_F}$-profiles correspond to the initial laminar profiles of the DNS at $t/t_f = 0$, and the Σ-profile is approximated from the $\overline{Y_F}$-profile through $\Sigma(y,0) = \overline{Y_F}(y,0)\left(1-\overline{Y_F}(y,0)\right) / \int_0^h \overline{Y_F}\left(1-\overline{Y_F}\right)\mathrm{d}y$.

The system is then free to evolve with the following boundary conditions:

at the wall ($y = 0$): $\overline{T}(0,t) = T_1$, $\partial\overline{Y_F}/\partial y\,(0,t) = 0$, $\Sigma(0,t) = 0$;

in the middle of the channel: $\overline{T}(h,t) = T_2$, $\overline{Y_F}(h,t) = 0$, $\Sigma(h,t) = 0$.

Results of the model are shown in figure 21 and compared with the DNS results.

The total reaction rate increases as the flame approaches the wall and is wrinkled by turbulence. The model compares well with the DNS and predicts acurately the decrease of mean total mass fraction and mean wall mass fraction of fuel, and the maximum of mean wall heat flux.

5. Conclusions

During turbulent flame–wall interaction, walls decrease the flame speed through enthalpy losses and lead to flame quenching but also to modifications of flame wrinkling. A three-dimensional constant-density simulation database created by direct numerical simulation (Bruneaux *et al.* 1996) has been used in this work to study these phenomena. The influence of the wall on flame propagation was investigated in terms of wall heat flux, flame speed and flame surface density transport.

A flamelet model able to describe free flame propagation as well as flame-wall interaction was derived. The starting point of the model is the exact interface density equation (Trouvé & Poinsot 1994; Candel & Poinsot 1990; Pope 1988). In this unclosed equation, all terms were measured by averaging the DNS results over 30 realizations and in planes parallel to the channel walls (directions of homogeneity). First, an exact budget for the flame surface density was closed to check the accuracy and the self-consistency of the DNS and of the model equation for flame surface density. Dominant terms were identified: for example, it was shown that during the interaction, large gradients of Σ near the wall created an inversion of the balance between the production–destruction terms and the transport terms. Then, each term was studied and modelled using DNS results. Wall corrections were introduced when needed.

Two types of tests were performed on the model.

(i) *A priori* tests: individual terms of the conservation equation for flame surface density as well as heat transfer terms were compared to DNS. The effects of enthalpy losses were introduced into a model for the consumption speed and validated against the DNS database. A closure for the Σ-equation including quenching effects and scale decrease in the vicinity of the wall was proposed and validated against DNS. It includes a model for the propagation term that takes into account the flame retreat from the wall. A budget for this corrected Σ-equation was then presented.

(ii) *A posteriori* tests, where the final model was used to compute the DNS configuration. Results of the model and DNS were compared in terms of total reaction rate, mean heat flux to the wall or mean unburnt mass fraction at the wall.

The final model constitutes an extension of existing flamelet models and matches the present DNS data far from and close to walls. Its validity in flows with higher Reynolds numbers or with large heat release (situations which are difficult to handle with DNS at the moment) has to verified in the future by comparing model predictions and experimental results.

The first author would like to thank the ADEME for its financial support, and NASA Ames and the Center for Turbulence Research for the computer time. Part of this work was done during the 1994 Summer Program of the Center for Turbulence Research. The help of Dr K. Akselvoll during the development of the code is gratefully acknowledged. This research was partly financed by the Commission of the European Communities within the framework of the Joule Program (JOU2-CT92-0162), by the Swedish National Board for Technical Development NUTEK, by the Austrian Government, by the Research Committee of European Automobile Manufacturers

(Fiat, Peugeot SA, Renault, Rover, Volkswagen and Volvo) within the IDEA EFFECT Program.

REFERENCES

Baum, M., Poinsot, T., Haworth, D. & Darabiha, N. 1994 Using direct numerical simulations to study $H_2/O_2/N_2$ flames with complex chemistry in turbulent flows. *J. Fluid Mech.* **281**, 1–32.

Boudier, P., Henriot, S., Poinsot, T. & Baritaud, T. 1992 A model for turbulent flame ignition and propagation in spark ignition engine. *24th Symp.* (*Intl*) *on Combustion*, pp. 503–510. The Combustion Institute.

Bray, K. N. C. 1990 Studies of the turbulent burning velocity. *Proc R. Soc. Lond.* A **431**, 315–335.

Bray, K. N. C., Libby, P., Masuya, P. & Moss, G. 1981 Turbulence production in premixed turbulent flames. *Combust. Sci. Technol.* **25**, 127–140.

Bruneaux, G., Akselvoll, K., Poinsot, T. and Ferziger, J. 1996 Flame-wall interaction simulation in a turbulent channel flow. *Combust. Flame* **107**, 27–44.

Candel, S. M. & Poinsot, T. 1990 Flame stretch and the balance equation for the flame surface area. *Combust. Sci. Technol.* **70**, 1–15.

Candel, S., Veynante, D., Lacas, F., Maistret, E., Darabiha, N. & Poinsot, T. 1990 Coherent Flame Model: applications and recent extensions. In *Recent Advances in Combustion* (ed. B. Larrouturou). World Scientific.

Cant, S., Pope, S. & Bray, K. N. C. 1990 Modelling of flamelet surface-to-volume ratio in turbulent premixed combustion. *23rd Symp.* (*Intl*) *on Combustion*, pp. 809–815. The Combustion Institute.

Clendening, J. C. W., Shackleford, W. & Hilyard, R. 1981 Raman scattering measurement in a side-wall quench layer. *18th Symp.* (*Intl*) *on Combustion*, pp. 1583–1589. The Combustion Institute.

Duclos, J-M., Veynante, D. & Poinsot, T. J. 1993 A comparison of flamelet models for premixed turbulent combustion. *Combust. Flame* **95**, 101–117.

Ezekoye, O. A. & Greif, R. 1993 A comparison of one and two dimensional flame quenching: heat transfer results. *Trans. ASME: Heat Transfer in Fire and Combustion Systems* **250**, 11–20.

Ezekoye, O. A., Greif, R. & Lee, D. 1992 Increased surface temperature effects on wall heat transfer during unsteady flame quenching. *24th Symp.* (*Intl*) *on Combustion*, p. 1465. The Combustion Institute.

Haworth, D. C. & Poinsot, T. J. 1992 Numerical simulations of Lewis number effects in turbulent premixed flames. *J. Fluid Mech.* **244**, 405–436.

Huang, W. M., Vosen, S. R. & Greif, R. 1986 Heat transfer during laminar flame quenching, effect of fuels. *21st Symp.* (*Intl*) *on Combustion*, pp. 1853–1860. The Combustion Institute, Pittsburgh.

Jarosinski, J. 1986 A survey of recent studies on flame extinction. *Combust. Sci. Technol.* **12**, 81–116.

Jennings, M. & Morel, T. 1990 A computational study of wall temperature effects on engine heat transfer. *SAE Paper* 910459.

Kays, W. M. & Crawford, M. E. 1993 *Convective Heat and Mass Transfer*, 3rd Edn, pp. 269–274. McGraw Hill.

Kim, J., Moin, P. & Moser, R. 1987 Turbulence statistics in fully developed channel flow at low Reynolds number. *J. Fluid Mech* **177**, 133–166.

Launder, B. E. & Spalding, D. B. 1972 *Mathematical Models of Turbulence*. Academic Press.

Lu, J. H., Ezekoye, O., Greif, R. & Sawyer, F. 1990 Unsteady heat transfer during side wall quenching of a laminar flame. *23rd Symp.* (*Intl*) *on Combustion*, pp. 441–446. The Combustion Institute.

Mantel, T. & Borghi, R. 1994 A new model of premixed wrinkled flame propagation based on a scalar dissipation equation. *Combust. Flame* **96**, 443–457.

Meneveau, C. & Poinsot, T. 1991 Stretching and quenching of flamelets in premixed turbulent combustion. *Combust. Flame* **86**, 311–332.

Poinsot, T. J., Haworth, D. C. & Bruneaux, G. 1993 Direct numerical simulation and modeling of flame-wall interaction for premixed turbulent combustion. *Combust. Flame* **95**, 118–132.

Pope, S. B. 1988 Evolution of surfaces in turbulence. *Intl J. Engng Sci.* **26**, 445–469.

Popp, P. & Baum, M. 1997 An analysis of wall heat fluxes, reaction mechanisms and unburnt

hydrocarbons during the head-on quenching of a laminar methane flame. *Combust. Flame* **108**, 327–348.

Rutland, C. 1989 Effects of strain, vorticity, and turbulence on premixed flame. PhD thesis, Stanford University, Stanford.

Rutland, C. & Cant, S. 1994 Turbulent transport in premixed flames. *Proc. Summer Program.* Center for Turbulence Research, Stanford.

Steiner, T. & Boulochos, K. 1995 Near-wall unsteady premixed flame propagation in S.I. engines. *SAE Paper* 951001.

Trouvé, A. & Poinsot, T. 1994 The evolution equation for the flame surface density in turbulent premixed combustion. *J. Fluid Mech* **278**, 1–31.

Trouvé, A., Veynante, D., Bray, K. N. C. & Mantel, T. 1994 The coupling between flame surface dynamics and species mass conservation in premixed turbulent combustion. *Proc. Summer Program*, pp. 95–124. Center for Turbulence Research, Stanford.

Vlachos, D. G. 1995 The interplay of transport, kinetic and thermal interactions in the stability of premixed hydrogen/air flames near surfaces. *Combust. Flame* **103**, 59–75.

Vlachos, D. G. 1996 Homogeneous-heterogeneous oxidation reactions over platinium and inert surfaces. *Chem. Engng Sci.* **51**, 2429–2438.

Vosen, S. R., Greif, R. & Westbrook, C. K. 1984 Unsteady heat transfer during laminar flame quenching. *20th Symp.* (*Intl*) *on Combustion*, pp. 76–83. The Combustion Institute.

Westbrook, C. K., Adamczyk, A. & Lavoie, G. 1981 A numerical study of laminar flame-wall quenching. *Combust. Flame* **40**.

Wichman, I. S. & Bruneaux, G. 1995 Head-on quenching of a premixed flame by a cold wall. *Combust. Flame* **103**, 296–310.

Williams, F. A. 1985 *Combustion Theory*, pp. 73–76. B. Cummings, Menlo Park, CA.